Science of the Total Environment 671 (2019) 1245–1256

Contents lists available at ScienceDirect

Science of the Total Environment

journal homepage: www.elsevier.com/locate/scitotenv

Using multiple tracers (F^-, B, $\delta^{11}B$, and optical brighteners) to distinguish between municipal drinking water and wastewater inputs to urban streams

Kayla A. Lockmiller [a], Kun Wang [b], David A. Fike [b], Andrew R. Shaughnessy [a,1], Elizabeth A. Hasenmueller [a,*]

[a] Department of Earth and Atmospheric Sciences, Saint Louis University, Saint Louis, MO 63108, United States
[b] Department of Earth and Planetary Sciences, Washington University in St. Louis, Saint Louis, MO 63130, United States

HIGHLIGHTS

- Tracers were used to assess drinking water and wastewater inputs to streams.
- Municipal waters have distinct tracer (F^-, B, $\delta^{11}B$, and optical brightener) values.
- Municipal water tracer levels were low in rural streams, but high in urban streams.
- Drinking water and wastewater respectively contribute up to 54% and 16% of flow.

GRAPHICAL ABSTRACT

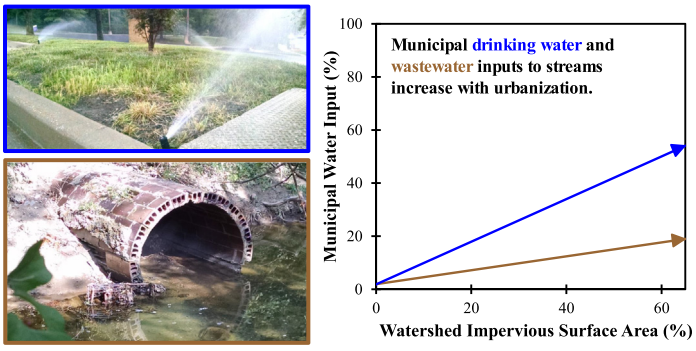

ARTICLE INFO

Article history:
Received 3 October 2018
Received in revised form 21 March 2019
Accepted 22 March 2019
Available online 25 March 2019

Editor: Ashantha Goonetilleke

Keywords:
Drinking water
Wastewater
Water sourcing
Urban streams
Chemical tracers
Water quality

ABSTRACT

Releases of municipal waters, including drinking water and wastewater, can considerably alter urban stream chemistry. However, the relative contributions of drinking water versus wastewater to streams have not been quantified previously and are therefore the focus of this study. We sampled streams along a land use gradient that included watersheds with impervious surface areas (ISA) ranging from 1.6 to 62.6%. Samples were analyzed for F^-, total B, $\delta^{11}B$, and optical brighteners to determine municipal water inputs to streams. We observed low F^- (75 ± 20 μg/L), B (29 ± 6 μg/L), and optical brightener (3.66 ± 0.76 RFU) levels in rural streams, but their concentrations increased with urbanization (up to 475 μg/L, 227 μg/L, and 22.09 RFU, respectively). The $\delta^{11}B$ values for drinking waters (16.52 ± 0.39‰) and wastewaters (untreated $= 6.06 \pm 0.88$‰ and treated $= 6.46 \pm 0.93$‰) were distinct, but there was poor correlation between $\delta^{11}B$ and ISA for the streams ($R^2 = 1 \times 10^{-5}$; $p = 0.99$), likely due to variable lithology in the study area. We used inverse and three-component mixing models to quantify municipal water inputs to the streams. In densely urbanized watersheds, drinking water and wastewater can respectively contribute up to 54% and 16% of the total streamflow. In addition to our spatial sampling, we collected weekly samples at a suburban stream to test the effects of discharge and seasonality on municipal water tracer behavior. We found that tracer levels did not change significantly ($p \geq 0.28$) with discharge or season, suggesting that municipal water inputs are fairly constant. Understanding the relative proportions of differing

* Corresponding author.
E-mail address: elizabeth.hasenmueller@slu.edu (E.A. Hasenmueller).
[1] Current affiliation: Department of Geosciences, The Pennsylvania State University, University Park, PA 16802, United States.

https://doi.org/10.1016/j.scitotenv.2019.03.352

municipal water types to streams is crucial in guiding infrastructure improvements to conserve drinking water and reduce harmful wastewater releases. The unique chemical signatures of municipal waters aid in the widespread applicability of our multi-tracer method for identifying water sourcing to urban streams.

1. Introduction

With over half of the world's population living in cities (UNDESA, 2016), municipal water use is leading to significant alteration of urban streams. Municipal waters (i.e., treated drinking water, treated wastewater, and untreated wastewater) may be released into proximal waterbodies through several mechanisms including over-irrigation of lawns with drinking water, discharges of treated wastewater, discharges of untreated wastewater from sewer overflows, and leaks from drinking water and wastewater infrastructure. Inputs of municipal waters to streams can profoundly influence water quality and quantity. However, it is often challenging to determine the amount of municipal water entering natural waterways because of the inherent difficultly in tracking irrigation rates, sewer overflows, and leaking infrastructure.

Previous workers have used geochemical multi-tracer approaches to identify water and contaminant sourcing to rivers and groundwaters impacted by urban and agricultural land uses (Widory et al., 2004a, 2004b; Chetelat and Gaillardet, 2005; Petelet-Giraud et al., 2009; Briand et al., 2013, 2017). However, a multi-tracer approach has not yet been applied to distinguish between municipal drinking waters and wastewaters. Indeed, there are several chemical species that can be unique to drinking (F^-) and wastewater (B, B isotopes, and optical brighteners in gray waters as well as K, artificial sweeteners, and pharmaceuticals in black waters) sources, which can be exploited as tracers to determine municipal water inputs to streams.

In industrialized countries, F^- is added to most drinking water supplies to promote dental health (Reardon and Wang, 2000; Kohn et al., 2001). Indeed, drinking water fluoridation occurs in 25 countries, with nearly 360 million people worldwide receiving artificially fluoridated water (Lennon et al., 2004; Cheng et al., 2007). In the United States alone, 66% of the population uses fluoridated drinking water (CDC, 2014). Moreover, F^- is a conservative tracer (Kennedy et al., 1991; Xu et al., 2016) that is not substantially altered from drinking water use nor is it removed in significant quantities during the wastewater treatment process (Meenakshi and Maheshwari, 2006). Concentrations of F^- have been used to trace the combination of drinking water and wastewater (i.e., total municipal water) inputs to southwestern United States streams. Here, it was determined that 25–60% of an urban stream's flow was derived from both municipal water types (Christian et al., 2011). It has also been used to trace municipal wastewaters alone. For example, F^- levels were used to establish that wastewater contributions made up ~8% of the total discharge in a midwestern United States stream (Stueber and Criss, 2005).

A common constituent of detergents and cleaning products is B (as $Na_2B_4O_7{\cdot}10H_2O$), where it is used as a bleaching agent (Vengosh et al., 1994; Henckens et al., 2015). Indeed, detergents and soaps account for 4% of the world's B consumption (USGS, 2012). This use of B leads to high concentrations in domestic and industrial wastewaters, ranging from several hundred μg/L to several mg/L (Barth, 2000; Fox et al., 2000). These characteristically high B concentrations have been used in studies that address wastewater inputs to natural waters (Butterwick et al., 1989; Barth, 1998; Stueber and Criss, 2005; Guinoiseau et al., 2018).

Likewise, B isotopic ratios ($\delta^{11}B$) have been exploited to determine wastewater inputs to streams and groundwater. Nearly 90% of B used in detergents is sourced from two deposits of sodium perborate minerals: one in California, United States, and the other in Western Turkey (Barth, 1998). Both of these deposits feature low $\delta^{11}B$ values, ranging from −0.9 to 10.2‰ in the United States and −5.4 to −1.7‰ in Turkey (Barth, 1998). Researchers have found similar $\delta^{11}B$ values among sampled wastewaters (Vengosh et al., 1994; Barth, 1998; Widory et al., 2005; Guinoiseau et al., 2018), which range from −2.4 (Guinoiseau et al., 2018) to 12.9‰ (Vengosh et al., 1994). These well-established, characteristically low, isotopic ratios in wastewaters, combined with the fact that the sources and fluxes of B in the global B cycle are well-constrained and equilibrated (Guinoiseau et al., 2018 and references therein), make $\delta^{11}B$ ideal for tracing municipal waters. For example, B isotopes, along with B concentrations, have demonstrated that municipal waters contribute as much as 70 ± 20% to the total volume of the Seine River in highly urbanized areas of France (Chetelat and Gaillardet, 2005). Guinoiseau et al. (2018) examined the same river over a 15 year period and observed that the B concentrations and isotopic signatures of municipal waters discharging to the Seine River changed over time due to the replacement of perborates with percarbonates in detergents. Nevertheless, Guinoiseau et al. (2018) found that the total municipal water contributions to the river were similar to previous estimates by Chetelat and Gaillardet (2005), and thus B isotopes remained a good tracer of municipal water inputs.

Optical brighteners have also been used to assess wastewater inputs to aquatic systems. These compounds are stilbene-type fluorescent whitening agents (FWA) that increase the brilliance of clothing and paper products by absorbing ultraviolet light, usually at 340–370 nm, and reemitting it as blue light, usually at 420–470 nm (Tavares et al., 2008; Gholami et al., 2016). Optical brighteners are added to 97% of detergents in the United States and most types of toilet paper (Tavares et al., 2008; Gholami et al., 2016), and are consequently found in high concentrations (up to 22 μg/L) in wastewaters (Hayashi et al., 2002; Cao et al., 2009). Hayashi et al. (2002) found relatively high concentrations of optical brighteners (up to 6.4 μg/L) in highly urbanized streams and coastal areas in Japan, likely due to additions from wastewater effluents and leaking wastewater infrastructure. Since these compounds are largely removed during wastewater treatment (i.e., 55–98% reduction) due to their affinity to sewage sludge (Poiger et al., 1998), optical brighteners are an effective tracer for untreated wastewaters from leaking wastewater infrastructure and sewer overflow inputs.

Previous work tracing municipal water contributions to urban streams has focused on determining only one end-member, like wastewater, or a combination of end-members (i.e., total municipal inputs) to streamflow. Thus, researchers generally only use one or two tracers that are characteristic of municipal waters. To our knowledge, no work has been done in separately quantifying both drinking water and wastewater contributions to streams using chemical tracers. This is surprising given the common use of fluoridated drinking water in industrialized countries and additions of various chemical species, like B (with a characteristic isotopic signature) and optical brighteners from laundry detergents, during use. It is important to separately quantify drinking water and wastewater contributions to streams as their chemistries are vastly different and have varying impacts on natural systems. Thus, this work distinguishes between drinking water and wastewater fractions in urban streams using a suite of geochemical tracers, including dissolved F^-, total B, $\delta^{11}B$ values, and optical brighteners, as well as inverse and three-component mixing models. We found that municipal water inputs increased with urbanization. In the most densely urbanized watersheds we sampled, drinking water and wastewater represent up to 54% and 16% of the total streamflow, respectively. Our method can be applied in areas that feature these tracers in municipal

waters or used to help constrain municipal end-member inputs to streams in regions where municipal water types may not feature distinct chemical signatures (e.g., locations without fluoridated drinking water).

2. Material and methods

2.1. End-member selection and study location

For this study, we considered three separate possible end-member contributions to urban streams in Saint Louis, Missouri, United States. They include: (1) the unaltered (hereafter referred to as "natural") input of groundwater as baseflow to streams, represented by rural streams ~40 km west of downtown Saint Louis that are predominantly forested and feature low watershed impervious surface area (ISA) values of <2%, (2) municipal drinking water inputs, represented by treated drinking water derived from chemically unique Missouri River water (Criss et al., 2001; Hasenmueller and Criss, 2013; see Supplemental Material Section 1.1 for more details about drinking waters), and (3) municipal wastewater inputs, represented by wastewater treatment plant influents and effluents derived from Missouri River-type drinking waters (see Supplemental Material Section 1.2 for more details about wastewaters). Other possible sources of our tracers of interest, including atmospheric deposition, fertilizers, and road deicing salts, were excluded from our study as they were not found to be important contributors in this region (Hasenmueller and Criss, 2013).

To quantify the inputs of each of the aforementioned end-members to streams in our study area, we sampled 18 watersheds at 65 locations (Fig. 1). All of the streams we sampled are within the region where Missouri River-type drinking water is distributed (Jordan, 1965; Missouri American Water, 2016; see black outline in Fig. 1). The subwatersheds draining to each selected stream site represent a gradient of land use (Homer et al., 2015) from 1.6 to 62.6% ISA (Xian et al., 2011; Fig. 1). We used ISA as a proxy for the density of water infrastructure because water infrastructure location data were unavailable for security reasons (see Supplemental Material Section 2.1 for details on the ISA calculation method). 31562Some of the urban streams (i.e., ISA values generally >30%) in our study are highly altered and feature long stretches of concrete channel linings (up to several kilometers) with sparse riparian vegetation (Hasenmueller and Robinson, 2016; Hasenmueller et al., 2017). The rural streams selected for this study receive higher baseflow contributions, are less flashy during floods, and are typically more densely vegetated along their banks than their urban counterparts (Hasenmueller et al., 2017). Regional lithology consists of Ordovician dolostones and Carboniferous limestones and shales.

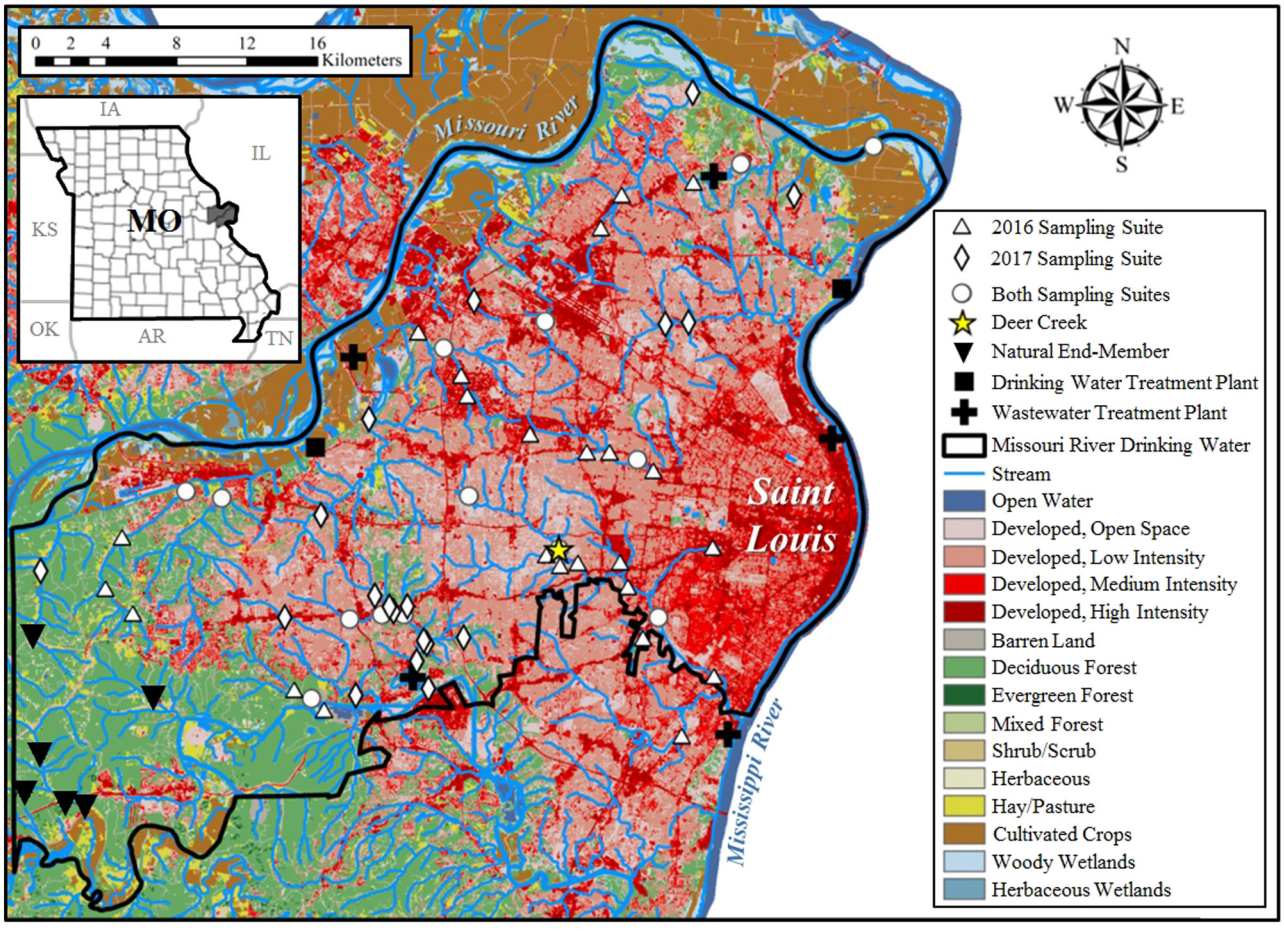

Fig. 1. Stream and end-member sampling locations in Saint Louis, Missouri, on a land use/land cover map (Homer et al., 2015). The black outline represents the area in which Missouri River-derived drinking water is distributed (Missouri American Water, 2016). Stream sampling locations were visited September to December 2016 (white triangles), September 2017 (white diamonds), or during both sampling periods (white circles). Our weekly sampling location, Deer Creek, is indicated with a yellow star (note that this symbol overlies a white circle as this site was also sampled during our 2016 and 2017 field campaigns). The watersheds with the lowest (i.e., <2%) ISA in the study area represent our natural end-member (black inverted triangles). Data collected from drinking water (black squares) and wastewater (black crosses) treatment plants represent the chemical character of our municipal end-members. Note that one of Saint Louis' drinking water treatment plants draws directly from the Missouri River, while the other is located on the western bank of the Mississippi River, just below the confluence with the Missouri River. Although the second treatment plant is not situated directly on the Missouri River, it still treats Missouri River-type water under normal flow conditions due to slow river mixing processes below the confluence (Jordan, 1965).

2.2. Sample collection

Stream samples ($n = 81$) were collected during two separate sampling events at the 65 stream sites across the land use gradient (Fig. 1). Stream sites with low ISA (<2%; six locations in three watersheds) were used to determine the natural end-member ($n = 8$). Samples were also collected to characterize the municipal water end-members (Fig. 1) including: 1) Missouri River water prior to drinking water treatment near two drinking water treatment plants ($n = 6$), 2) treated drinking water sourced from the Missouri River from two drinking water treatment plants ($n = 5$), and 3) untreated ($n = 6$) and treated ($n = 6$) wastewater from five wastewater treatment plants that receive drinking water derived from the Missouri River (only the wastewater treatment plants that receive Missouri River-type drinking water were selected as not to convolute analysis of the wastewater end-member signature with wastewaters derived from other drinking water sources). Stream and end-member samples were collected from September through December 2016 ($n = 54$) and in September 2017 ($n = 50$). Some stream locations were sampled in both collection suites ($n = 15$), while others were sampled only once to build the spatial density of water quality data. Over 50% of the sites were close (<1 km) to United States Geological Survey (USGS) gauging stations (USGS, 2018) so that chemical data could be compared with discharge data. To avoid introducing another end-member (i.e., runoff from recent precipitation events), all stream samples were taken at baseflow conditions. We define baseflow as flow conditions near the seasonal average for the stream of interest (USGS, 2018) and that occur at least 3 days after a precipitation event.

At each site and for both sampling events, in situ results for standard water quality parameters were measured with a YSI Professional Plus Multiparameter Instrument (temperature, dissolved oxygen (DO), specific conductivity, and pH) and Hach 2100P Portable Turbidimeter (turbidity); these instruments were calibrated with known standards before field visits. Aliquots for ion chromatography (IC) and inductively coupled plasma optical emission spectrometry (ICP-OES) were field-filtered through 0.2 μm cellulose acetate filters into polypropylene (PP) vials; subsamples to be run with an ICP-OES were acidified to 1% HNO_3. Both sample types were kept on ice until returning to the lab where they were stored at 4 °C until analysis. During the September 2017 sampling event, measurements for optical brighteners (presented in relative fluorescence units (RFU)) were also made on site using a Turner Designs AquaFluor Handheld Fluorometer in UV grade methacrylate cuvettes. The fluorometer was calibrated with known standard solutions prior to field excursions. Subsamples for $\delta^{11}B$ ($n = 31$) were also collected from select sites in PP vials during the second sampling suite. Sites selected for B isotope analysis represented all three end-members and watershed ISA ranging from 1.6 to 47.1%. These samples were filtered, but not acidified, and frozen until analysis.

In addition to the two main sampling events during low water periods, samples were collected approximately weekly (from September 2016 to March 2018; $n = 61$) at a suburban stream (i.e., Deer Creek; ISA = 28.0%; yellow star on Fig. 1) with known wastewater inputs from a combined sewer overflow (CSO; MSD, 2017) and drinking water contributions from nearby lawn irrigation. This stream acts as a control to observe the effects of discharge and seasonality on municipal water tracer behavior. All of the same in situ water quality measurements were made at this site. We also collected aliquots for F^- and B during the entire study period. Optical brightener levels were measured from September 2017 to March 2018. Due to resource limitations, we collected only one $\delta^{11}B$ sample in September 2017 during baseflow conditions.

2.3. Lab analyses

We used a Metrohm 881 Compact IC Pro Ion Chromatograph with a Metrosep A Supp 7 column with suppression to measure F^- and other anions on a conductivity detector. An eluent of 3.6 mM Na_2CO_3 was used at a flow rate of 0.7 mL/min. Total B and major cations were analyzed on a PerkinElmer Optima 8300 ICP-OES with Fluka Analytical Multi-Element Standard Solution 1. Replicates, blanks, and check standards were run on both instruments to test the reliability of field and lab techniques. Accuracy and precision were within 5.0% for all analytes for both the IC and ICP-OES measurements. The $\delta^{11}B$ sample subset was processed following previously outlined methods (Guerrot et al., 2010). Briefly, samples were purified through columns filled with Amberlite IRA-743 boron-specific resin and then run on a Neptune Plus multi-collector inductively coupled plasma mass spectrometer (MC-ICP-MS) bracketed with the NIST SRM 951 standard; accuracy and precision were within 0.1‰ (additional $\delta^{11}B$ method details are provided in Supplemental Material Section 2.2).

2.4. Mixing models to quantify municipal end-member inputs to streams

We tested two mixing models to quantify the relative contributions of the end-members to streams across the study area. Both models assume conservative mixing between end-members. The conservative behavior of many of our analytes (e.g., F^-, B, $\delta^{11}B$, and Ca) has previously been demonstrated (see Kennedy et al., 1991; Negrel et al., 1993; Roy et al., 1999; Guinoiseau et al., 2018). We selected the 2017 sampling suite for our end-member mixing analyses because more tracer data were available (e.g., optical brightener and $\delta^{11}B$ data).

We modeled the contributions of municipal waters and natural water through baseflow using the mass-balance equation:

$$Q_S C_S = Q_D C_D + Q_W C_W + Q_N C_N \quad (1)$$

where the subscripts S, D, W, and N respectively represent the stream of interest and end-member (i.e., drinking water, wastewater, and natural water) discharge (Q) or tracer concentration (C). Dividing both sides of the equation by Q_S yields:

$$C_S = \alpha_D C_D + \alpha_W C_W + \alpha_N C_N \quad (2)$$

where $\alpha_i = \frac{Q_i}{Q_S}$ and is the proportion of water sourced from end-member i (i.e., drinking water, wastewater, or natural water). Additionally, we constrained the system so that the sum of the mixing proportions equals 1:

$$1 = \alpha_D + \alpha_W + \alpha_N \quad (3)$$

Following the work of previous researchers (e.g., Negrel et al., 1993; Roy et al., 1999; Gaillardet et al., 1999; Chetelat and Gaillardet, 2005; Guinoiseau et al., 2018), we first solved the system using an inverse method, where $C = F^-$, total B, optical brighteners, Ca^{2+}, Mg^{2+}, K^+, NO_3^-, and SO_4^{2-}. We did a second calculation with the inverse mixing model using those same analytes as well as $\delta^{11}B$ values. We omitted Na^+ and Cl^- as tracers for the inverse mixing model due to the pervasive use of NaCl as a road deicer in the winter months in our study area; this contamination especially impacts the more urbanized streams (Hasenmueller and Criss, 2013; Hasenmueller and Robinson, 2016; Hasenmueller et al., 2017; Robinson et al., 2017; Robinson and Hasenmueller, 2017). Because there are three unknowns and nine (i.e., the first inverse model calculation) or ten (i.e., the second inverse model calculation) equations, the system is over-constrained. Thus, we solved the inverse mixing model using a least-squares method. To account for uncertainties in the end-member compositions, 10,000 random end-member values were sampled from uniform distributions of end-member values. Then, 10,000 Monte Carlo simulations were calculated with the end-member combinations (Torres et al., 2016; Xu et al., 2016; Burke et al., 2018; Yin et al., 2019). As described in Torres et al. (2016), any models that yielded negative values for end-member proportions were treated as erroneous and removed. Additionally, we

assumed that there were no other end-members to the streams of interest. Thus, we removed any simulations where the mixing proportions did not sum to 1.00 ± 0.05. The remaining models were averaged for the final value.

We also tested the robustness of a three-component mixing model set forth by Lee and Krothe (2001) that uses fewer tracers to see if it yielded reliable results with only a few, easily measured analytes. The three-component mixing model uses Eqs. (1)–(3) and has three unknowns, but only three equations. Therefore, the end-member proportions could be simultaneously calculated in a matrix. We selected optical brighteners and F^- for the analysis because optical brighteners can be measured quickly and inexpensively in the field via fluorometry and IC technology for F^- analysis is widely available. Uncertainties in the three-component mixing model's predictions were calculated using the same Monte Carlo simulations described earlier.

3. Results and discussion

3.1. End-member characterization

The rural streams (watershed ISA < 2%) that acted as our natural end-member featured low concentrations of all the municipal water tracers we analyzed. Over both sampling suites, F^- concentrations averaged at 75 ± 20 μg/L, while the average B concentration was 29 ± 6 μg/L. Optical brighteners were analyzed only during our second sampling suite and had a value of 3.66 ± 0.76 RFU. A 2017 sample of our natural end-member had a $\delta^{11}B$ value of 12.76‰, while another similar rural stream (ISA = 2.7%) had a more enriched signature (16.58‰).

The municipal drinking water end-member consisted of samples from the two drinking water treatment plants that draw Missouri River-type water. Untreated source water had an average F^- concentration of 335 ± 155 μg/L, while the treated drinking water had an average F^- concentration of 626 ± 112 μg/L after F^- additions during treatment. Dissolved B concentrations averaged at 92 ± 13 μg/L in the source water and 82 ± 23 μg/L in the treated drinking water, indicating that little to no change in B levels occurs during treatment. Optical brightener values were low in the treated drinking water (5.52 ± 0.30 RFU). The $\delta^{11}B$ values for the Missouri River-type waters were distinct from other water types in the study, with the source water (17.06 ± 0.44‰) having a very similar composition to the treated water (16.52 ± 0.39‰), again suggesting little to no change in B during treatment (Table 1).

For the municipal wastewater end-member, we analyzed both treated and untreated wastewater samples collected from the five wastewater treatment plants in the study area. The average concentration of F^- was 560 ± 60 μg/L in raw, untreated wastewaters and 483 ± 56 μg/L in treated wastewaters, representing a ~14% reduction in F^- levels during treatment. Dissolved B concentrations were on average 212 ± 51 μg/L in the untreated wastewater influent and 213 ± 41 μg/L in the treated wastewater effluent (Table 1). The wastewater treatment process therefore does not significantly alter total B levels in the water, as has been shown by others (Hasenmueller and Criss, 2013; Guinoiseau et al., 2018). Wastewater B concentrations were ~2.5 times higher than drinking water values due to inputs of $Na_2B_4O_7 \cdot 10H_2O$ from detergents during use (Stueber and Criss, 2005; Hasenmueller and Criss, 2013). Optical brightener values in wastewaters were very high compared to natural waters and drinking waters. Untreated wastewaters had an average optical brightener value of 104.47 ± 38.69 RFU, while treated wastewaters had an average of 54.36 ± 9.93 RFU. This represents a 48% decrease in optical brightener levels during treatment, which is a lower reduction rate than was observed by Poiger et al. (1998). The most depleted $\delta^{11}B$ values were observed in the wastewater samples: untreated wastewaters had an average isotopic value of 6.06 ± 0.88‰ and treated wastewaters averaged at 6.46 ± 0.93‰, indicating little change in B isotopic composition with treatment.

3.2. Spatial trends for municipal water tracers in streams across a land use gradient

We found significant and positive correlations between levels of F^-, B, and optical brighteners and urbanization ($R^2 \geq 0.37$; $p < 0.01$; Table 1; Fig. 2). Specific conductivity and most other ion species were also positively correlated with ISA (Tables S1–S3). Rural streams (defined as streams with watershed ISA = 2–10%) featured low F^- values (average = 95 ± 27 μg/L) while urban streams (defined as streams with watershed ISA > 40%) had F^- values up to 475 μg/L (average = 291 ± 87 μg/L). Rural streams also contained low concentrations of B (25 ± 9 μg/L) and optical brighteners (9.43 ± 1.07 RFU). Urban streams had much higher B and optical brightener values at 91 ± 53 μg/L and 15.96 ± 3.94 RFU, respectively. We observed the weakest correlation between dissolved B and ISA because B concentrations increased rapidly in more urbanized streams (Fig. 2B). This potentially indicates that there are higher inputs of wastewaters relative to drinking waters in more densely populated areas. It is also possible that there are other sources of B in these catchments that we have not identified, though previous work by Hasenmueller and Criss (2013) indicates that sources such as atmospheric deposition, fertilizers, and road salts are likely not important inputs of B to urban streams.

We did not observe a correlation between $\delta^{11}B$ values and watershed ISA ($R^2 = 1 \times 10^{-5}$; $p = 0.99$; Fig. 2C). Nevertheless, the municipal end-members had distinctive B isotopic ratios that showed little variation among samples. Specifically, wastewaters had a characteristically depleted signature (untreated wastewaters = 6.06 ± 0.88‰; treated wastewaters = 6.46 ± 0.93‰) compared to drinking waters that had a more enriched signature of 16.52 ± 0.39‰ (Table 1). However, stream waters displayed a wider range in isotopic values. Our natural end-member had a $\delta^{11}B$ value of 12.76‰ (determined from one B isotope analysis), while streams with similarly low ISA (2–10%) had $\delta^{11}B$ values ranging from 13.39 to 16.58‰. Highly urbanized streams (ISA > 40%) also featured a wide range of $\delta^{11}B$ values from 11.84 to 19.62‰. Since the $\delta^{11}B$ values we observed do not follow similar trends as the other tracers (Fig. 2) and, in some cases, exceed the values of our end-members, we suspect a fourth end-member, perhaps lithology, may

Table 1
Municipal water tracer averages and standard deviations for end-members and streams across a land use gradient.[a]

Water type	n	F^- (μg/L)	Total B (μg/L)	$\delta^{11}B$ (‰)	Optical brighteners (RFU)
Untreated Missouri River water	6	335 ± 155	92 ± 13	17.06 ± 0.44	9.78 ± 1.20
Treated drinking water	5	626 ± 112	82 ± 23	16.52 ± 0.39	5.52 ± 0.30
Untreated wastewater	6	560 ± 60	212 ± 51	6.06 ± 0.88	104.47 ± 38.69
Treated wastewater	6	483 ± 56	213 ± 41	6.46 ± 0.93	54.36 ± 9.93
Natural stream water (ISA < 2%)	8	75 ± 20	29 ± 6	12.76	3.66 ± 0.76
Watershed ISA = 2–10%	6	95 ± 27	25 ± 9	14.99 ± 2.26	9.43 ± 1.07
Watershed ISA = 10–20%	7	163 ± 52	40 ± 17	19.48 ± 1.09	5.71 ± 1.25
Watershed ISA = 20–30%[b]	18	234 ± 43	48 ± 13	13.97 ± 2.94	13.90 ± 2.64
Watershed ISA = 30–40%	13	238 ± 62	59 ± 30	16.97 ± 1.82	14.29 ± 3.16
Watershed ISA > 40%	30	291 ± 87	91 ± 53	15.34 ± 3.04	15.96 ± 3.94

[a] Additional data for end-member and stream samples can be found in Tables S1–S3 and Lockmiller (2018).
[b] Note that an average of 61 samples from Deer Creek (collected 2016–2018) was used in this category as not to skew the data towards one monitoring site.

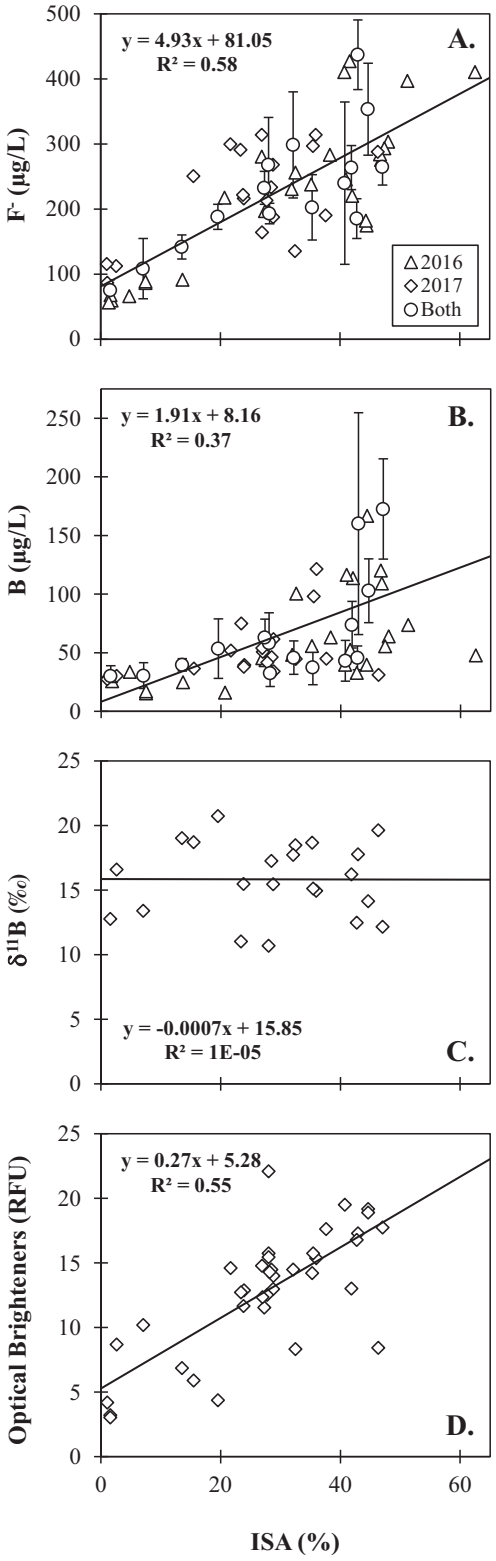

Fig. 2. Values for (A) F^-, (B) B, (C) $\delta^{11}B$, and (D) optical brighteners in streams plotted against watershed ISA. Data points represent stream samples collected in 2016 (white triangles), 2017 (white diamonds), or both (white circles; the average and standard deviation for the two sampling periods are indicated). The F^- and B samples were collected in 2016 and 2017, while $\delta^{11}B$ and optical brighteners were only analyzed for the 2017 sampling suite. There is a significant ($p < 0.01$) increase in F^-, B, and optical brighteners levels as ISA increases. Note the change in slope in B concentrations for ISA values of ~30% or more, which is likely related to higher wastewater inputs in the most urbanized streams. We did not see a correlation between $\delta^{11}B$ values and watershed ISA ($R^2 = 1 \times 10^{-5}$; $p = 0.99$).

be influencing the $\delta^{11}B$ ratios in Saint Louis-area streams. To assess the role of lithology, we compared samples collected from less developed watersheds with low densities of municipal water infrastructure, thus reducing the convoluting influence of the municipal water end-members. In low development watersheds underlain by Ordovician dolostones and lower Mississippian limestones, $\delta^{11}B$ values tended to be more depleted, while similarly rural watersheds in upper Mississippian limestones and Pennsylvania shales tended to have more enriched $\delta^{11}B$ values. Other studies have noted large differences in $\delta^{11}B$ values between sedimentary rock types. For example, Guinoiseau et al. (2018) noted that limestones from the Jura Mountains in France had $\delta^{11}B$ values of 10.0‰, while Noireaux et al. (2014) observed that shales in the Appalachian Mountains of the United States had $\delta^{11}B$ values of −4.5‰. However, these trends are the reverse of what we observe for carbonates and shales in the Saint Louis region. Because both land use and lithologic gradients occur across our study area, future work is needed to characterize the $\delta^{11}B$ values for various rock types in this region to better understand what impact they have on the composition of the natural water end-member.

To visualize the unique chemistries of our end-members and their impacts on our streams of interest, we created mixing diagrams using the F^-, B, $\delta^{11}B$, and optical brightener data (Fig. 3). The location of each stream plotted in Fig. 3 gives a relative sense of the contributions of each water type to the total flow. For the B and F^- (Fig. 3A) and optical brightener and F^- (Fig. 3B) mixing diagrams, we only considered the chemistry of untreated wastewaters for the municipal wastewater end-member because our study streams do not receive any treated effluents (Supplemental Material Section 1.2) and optical brightener levels can change considerably during the treatment process (Table 1). For the $\delta^{11}B$ mixing diagrams (Fig. 3C,D), we considered the chemistries of both treated and untreated wastewaters because not all of the untreated wastewater samples were analyzed for $\delta^{11}B$ and there is not a large change in B chemistry during the treatment process (average absolute value of change of 0.40‰ for $\delta^{11}B$ and 1 µg/L for B concentration; Table 1).

Stream F^-, B, and optical brightener values nearly all plot within the mixing triangles presented in Fig. 3A,B, implying that the natural and municipal end-members are the main contributors of these tracers. The rural stream chemistries fall closer to our natural end-member, while the urban streams plot near the drinking water and wastewater end-members. However, when the $\delta^{11}B$ values are considered, >60% of the stream samples plot outside of the mixing triangles (Fig. 3C,D). Given the large number of outliers for the B isotope mixing diagrams, it is likely that our single $\delta^{11}B$ sample of the natural end-member does not adequately represent its chemistry. In addition, the wide range in $\delta^{11}B$ values for streams with ISA < 20% again suggests that the variable lithology in our study area may influence the B isotopic signature of the natural end-member.

3.3. Relative fractions of municipal water inputs to streams

We quantified the relative fractions of drinking water (α_D), untreated wastewater (α_W), and natural water (α_N) in our stream sites using both the inverse and three-component mixing models and data from our 2017 sampling campaign. We only considered the chemistry of untreated wastewaters for the municipal wastewater end-member because our study streams do not receive any treated effluents (Supplemental Material Section 1.2) and optical brightener levels change during the treatment process (Table 1). We ran two tests for the inverse mixing model. The first test used molar concentrations of F^-, total B, Ca^{2+}, Mg^{2+}, K^+, NO_3^-, and SO_4^{2-} and optical brightener data, while the second test used the same analytes and $\delta^{11}B$ values (Table 2). For the three-component mixing model, we selected F^- and optical brightener data (Table 2) as these constituents are easily measured in streams and do not fall outside of the bounds of their mixing triangle (Fig. 3B). This

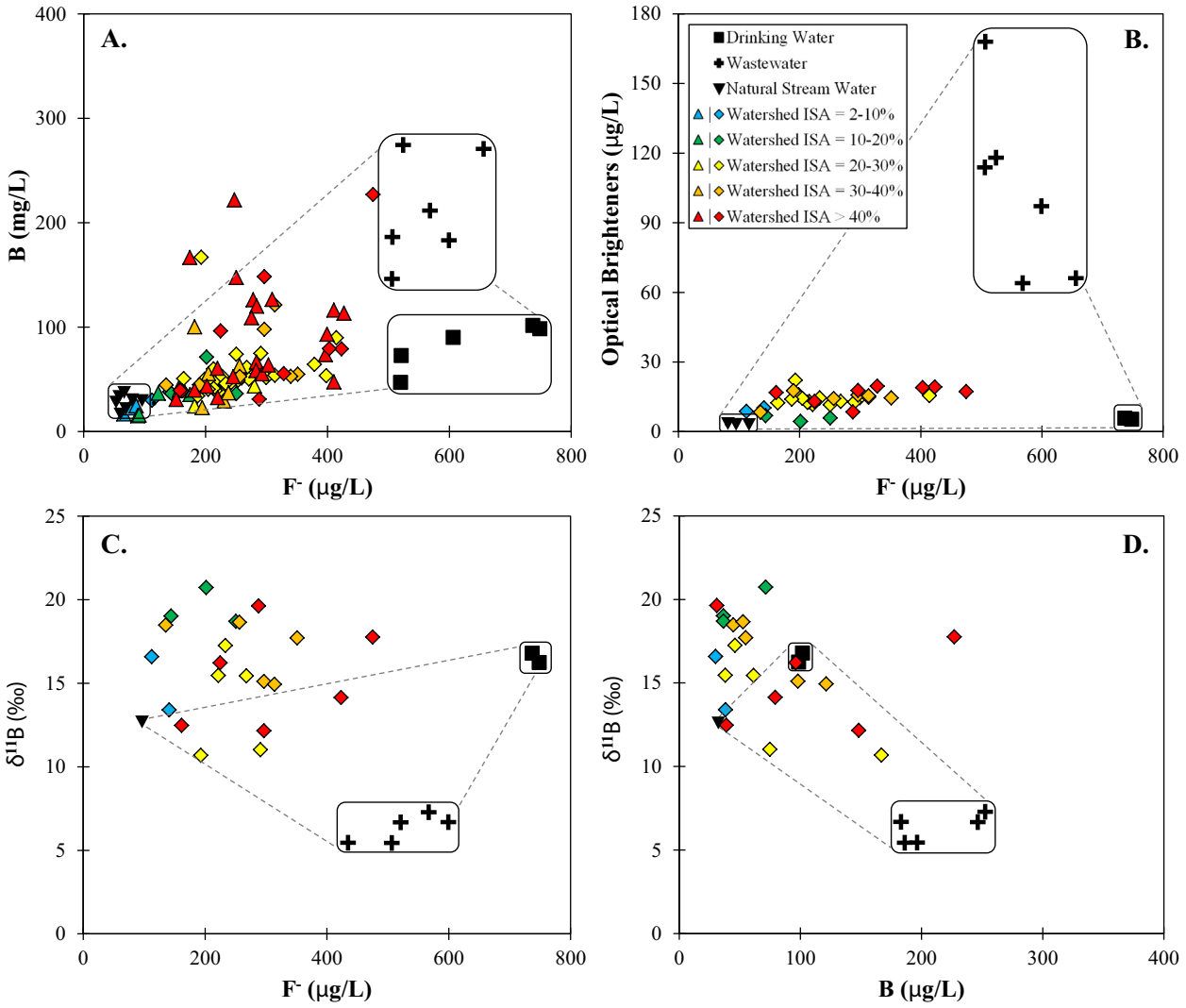

Fig. 3. Mixing diagrams for the drinking water (black squares), wastewater (black crosses), and natural water (i.e., watershed ISA < 2%; black inverted triangles) end-members and streams (triangles for 2016 data and diamonds for 2017 data; colors indicate the level of watershed ISA). Plots include: (A) B and F^-, (B) optical brighteners and F^-, (C) $\delta^{11}B$ and F^-, and (D) $\delta^{11}B$ and B chemistries. The variability in end-member compositions are highlighted with boxes. Note that there is only one sample for the natural water end-member for $\delta^{11}B$.

indicates that additional end-members either do not affect or minimally influence these analytes in streams.

In the first test of the inverse mixing model, we converged on apportioned end-member results for most of our sites (~70%), indicating that the model reasonably accounts for the end-member inputs to the streams. In this test, we found that drinking water and wastewater contributions to streams had positive and significant correlations with ISA ($R^2 \geq 0.65$ and $p < 0.01$ in both cases; Fig. 4A,B). Our calculations show that, combined, municipal waters may comprise as much as 66% of the total flow in urban streams. Drinking water made a more significant contribution to the total streamflow than did wastewater, supplying up to 54% of the flow in highly urbanized streams, while wastewaters contributed up to 16% (Fig. 4A,B). Less urbanized streams (i.e., ISA < 20%) featured lower municipal water inputs, with an average of 10 ± 8% of the flow being derived from drinking water and an average of 3 ± 2% of the flow being derived from wastewaters. Natural water contributions to streams through baseflow decreased significantly with increasing watershed ISA ($R^2 = 0.76$ and $p < 0.01$; Fig. 4C).

We ran a second test of the inverse mixing model, which included the same stream chemistries as the first model, but also our $\delta^{11}B$ values. However, when we included the $\delta^{11}B$ data in the model, the model generally (>50% of the stream sites) could not converge on answers that gave all positive proportions. The failure of the inverse mixing model to converge on apportioned end-member results, particularly when

Table 2
End-member compositional ranges used in the mixing models.[a]

Water type	F^- (mM)	Total B (mM)	$\delta^{11}B$ (‰)	Optical brighteners (RFU)	Ca^{2+} (mM)	Mg^{2+} (mM)	K^+ (mM)	NO_3^- (mM)	SO_4^{2-} (mM)
Treated drinking water	0.027–0.039	0.004–0.008	16.24–16.79	5.31–5.73	0.4–0.7	0.3–1.0	0.12–0.15	0.030–0.180	0.9–2.0
Untreated wastewater	0.027–0.035	0.014–0.025	5.43–6.68	63.90–168.00	0.7–1.1	0.6–1.1	0.27–0.41	0.002–0.140	1.0–2.7
Natural stream water	0.003–0.006	0.002–0.004	12.76	3.13–4.20	1.6–2.4	0.6–1.0	0.07–0.09	0.003–0.050	0.1–0.4

[a] Analyte averages for the end-members can be found in Tables 1, S1–S2 (note that these tables include all data, while only 2017 data are given here). Data for individual end-member and stream samples can be found in Table S3 and Lockmiller (2018).

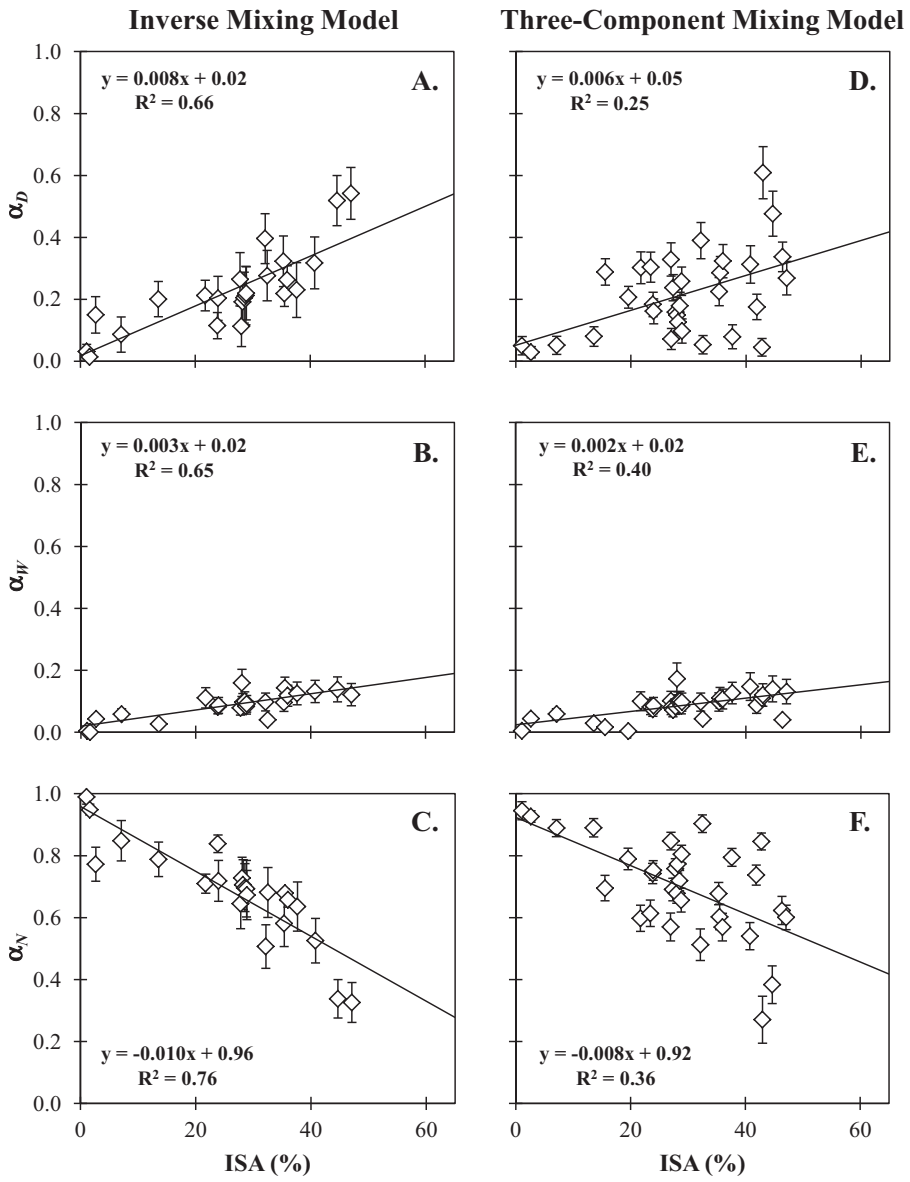

Fig. 4. Fractions of drinking water (α_D), untreated wastewater (α_W), and natural water (α_N) that comprised total streamflow, calculated with the inverse (A–C) and three-component (D–F) mixing models, are shown as a function of watershed ISA (a comparison of the models can be found in Fig. S1). The same streams are shown in each end-member contribution plot. As ISA increased, contributions of municipal waters increased and natural water decreased. Drinking water contributions were generally higher than wastewater inputs. All of the trends are significant ($p < 0.01$). The uncertainties for each calculated end-member input are shown. Note that in some cases the inverse mixing model could not converge on all positive values for the apportioned end-member contributions to a given stream.

using the B isotope data, could be the result of over-constraining the system or the narrow ranges for some of the end-member chemistries (Table 1, Fig. 3). Given the high variability in $\delta^{11}B$ values observed in the less developed streams (Fig. 3C,D), we also suspect that our data do not adequately characterize the natural end-member B isotope chemistry. We surmise that a fourth end-member (likely lithology) is influencing the $\delta^{11}B$ values in our study area. Future work is needed to constrain the impact of lithology on stream $\delta^{11}B$ values for this region.

Finally, we tested a simple three-component mixing model using easily obtained F^- and optical brightener data. For this mixing model test, we were able to converge on answers for all of the apportioned end-member results for each stream. With increasing ISA, the three-component mixing model demonstrated the same overall increasing trends in the municipal water end-members ($R^2 = 0.25$ for the drinking water end-member and $R^2 = 0.40$ for the wastewater end-member; $p < 0.01$ in both cases; Fig. 4D,E). The three-component mixing model showed that total municipal water inputs to streams may comprise up to 73% of the flow in the most urbanized streams sampled (compared to 66% for the first test of the inverse mixing model). Like the inverse mixing model, the three-component mixing model also demonstrated that drinking water made a more significant contribution to the total streamflow than did wastewater, supplying up to 61% of the flow in highly urbanized streams, while wastewaters contributed up to 17% (Fig. 4D,E). Less urbanized streams (ISA < 20%) featured low municipal water inputs, with an average of 12 ± 11% of flow being derived from drinking water and an average of 3 ± 2% of flow being derived from wastewater. The three-component mixing model results also showed that inputs of the natural end-member to streams decreased significantly with ISA ($R^2 = 0.36$; $p < 0.01$; Fig. 4F).

Overall, the calculated end-member contributions to streams were similar for both the inverse and three-component mixing models (Fig. 4). However, the R^2 and p values were lower and higher, respectively, for the three-component mixing model compared to the inverse mixing model. This is likely because the inverse mixing model assesses a

greater number of chemistries than does the three-component mixing model. Nevertheless, the three-component mixing model uses fewer tracers but still yields similar end-member inputs. This model was also able to converge on apportioned end-member inputs more frequently than either of the inverse mixing model tests. This is likely due to over-constraining the system for the inverse mixing model. Consequently, the three-component mixing model could be an ideal method for municipal water managers to quickly assess the relative proportions of the municipal end-member types (particularly wastewaters which demonstrated the highest R^2 and lowest p values) given its simplicity.

When the apportioned end-member results from each model were plotted together (Fig. S1), the best fit line slopes were close to unity and the intercepts were close to zero for each end-member; all of the R^2 values were > 0.78. We also calculated the values for each of the end-member samples using both the inverse and three-component mixing models to determine the recoveries for the two models (Fig. S1). For the drinking water and natural water end-members, recoveries were close to 100% for each water type. However, recoveries for the wastewater end-member averaged at ~70%. The lower recovery for the wastewater end-member observed in both models is likely the result of the large compositional range in the wastewater end-member (Fig. 3). Variable wastewater chemistries can be attributed to differences in use in the services areas.

3.4. Sourcing of municipal water contributions to streams

The higher contributions of drinking water calculated with both the mixing models are likely due to leaking pipes and possibly also runoff from lawn irrigation (Grimmond and Oke, 1986; Lerner, 2002; Passarello et al., 2012; Hasenmueller and Criss, 2013). Drinking water pipes are over-pressured, unlike wastewater pipes, which could lead to a greater leakage volume, especially in urban areas where pipe densities are highest. Indeed, estimates of leakage rates from drinking water pipes in developed countries typically range from 8 to 24% (Motiee et al., 2007) of the total volume of water carried by piping systems, though higher losses of 20–30% were observed in Austin, Texas, United States (Passarello et al., 2012). Though drinking water infrastructure leakage data for the Saint Louis area are unavailable, we suspect that water losses could be similar to Austin since estimates for the age of water-related infrastructure in both cities average around 55 years (Christian et al., 2011; ASCE, 2018). Additionally, commercial and residential lawn irrigation consumes nearly 34 billion liters of potable water daily in the United States alone, much of which is lost via surface runoff and infiltration due to excessive application (USEPA, 2018a). However, results from our temporal monitoring site (see Section 3.5) suggest that lawn irrigation may be a less important source of drinking water.

Untreated wastewater inputs to urban streams are likely due to contributions from leaking, antiquated wastewater infrastructure and discharges from CSOs, which only occur in the more urbanized areas of Saint Louis (MSD, 2017). Wastewater exfiltration rates range from 5 (Passarello et al., 2012) to 52% (Eiswirth and Hötzl, 1997) of the total volume carried in pipes, but many studies agree with more conservative losses (Barrett et al., 1997; Ellis et al., 2003; Vollertsen and Hvitved-Jacobsen, 2003; Rutsch et al., 2006; Christian et al., 2011). It has been noted that leaking infrastructure can contribute wastewater to streams as well as the shallow groundwater, which, in turn, feeds streams during baseflow conditions (Passarello et al., 2012). Furthermore, during times of moderate to heavy rainfall, urban streams in our study area experience discharges from CSOs with volumes exceeding 50 billion liters annually (USEPA, 2018b). However, the exact discharge amounts during wet weather conditions for specific CSOs were not available for this study.

Studies have found wastewater contributions to streams that range from 8 to 90% (Chetelat and Gaillardet, 2005; Stueber and Criss, 2005; Graham et al., 2014) of the total streamflow. Our average result for wastewater inputs to streams (9 ± 4%) falls on the lower end of this spectrum. However, other studies (e.g., Stueber and Criss, 2005; Christian et al., 2011) did not consider inputs from drinking water in their estimates, despite distinct differences between their drinking water and wastewater end-members. Additionally, our estimates for wastewater inputs to streams may represent a minimum value, as optical brighteners are subject to photo-decay over time. In detail, there are two common types of FWA used as optical brighteners, FWA-1 (disodium 4,4′-bis[(4-anilino-6-morpholino-1,3,5-trizin-2-yl)amino] stilbene-2,2′-disulphonate) and FWA-5 (benzenesulfonic acid, 2,2′ ([1,1′-biphenyl]-4,4′-diyldi-2,1-ethenediyl) bis-disodium salt), which are added to most detergents (Hagedorn et al., 2005; Gholami et al., 2016). Optical brighteners FWA-1 and FWA-5 are included in detergents in different concentrations (0.05–0.15% and 0.02–0.10% of the detergent formula, respectively) and each has a differing rate of photo-decay (Hagedorn et al., 2005). Specifically, FWA-1 decays more slowly, at ~50% degradation in 12 months, than FWA-5, which decays by approximately 70% in 28 days (Hagedorn et al., 2005). Based on this information, our wastewater input calculations may represent a minimum value for our streams. In addition, organic matter in natural and municipal wastewaters can interfere with fluorometric analysis of optical brightener levels. Future work is needed to assess these interferences in natural and municipal water samples.

As the relative proportions of municipal waters increase in streams, the fractions of natural water decrease. Indeed, in highly urbanized

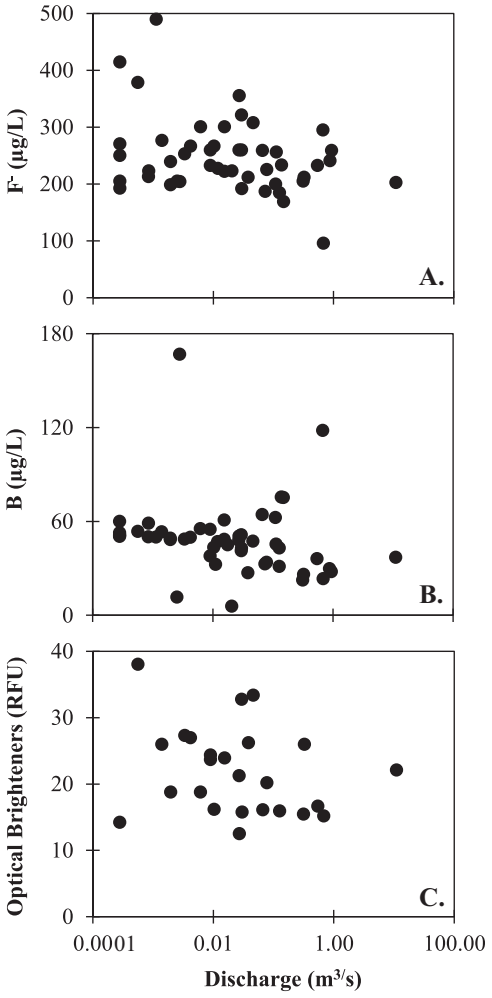

Fig. 5. Levels of (A) F^-, (B) B, and (C) optical brighteners plotted against discharge for our temporal monitoring site, Deer Creek. These tracers behave chemostatically ($R^2 \leq 0.01$; $p \geq 0.28$) over the sampling period, likely indicating concomitant increases in municipal waters with increased discharge.

streams, the natural water end-member may only represent 34% of the total streamflow. Nevertheless, we acknowledge that because both land use and lithologic gradients occur across our study area, future work is needed to characterize the variability in the natural end-member.

3.5. Temporal trends in municipal water inputs to a suburban stream

We monitored a small, suburban stream (Deer Creek; ISA = 28.0%; yellow star on Fig. 1) from September 2016 to March 2018 to determine temporal variations in municipal water inputs as a control for our study. Deer Creek's F^- and B concentrations fluctuated 96–490 μg/L (average = 252 ± 64 μg/L; Fig. 5A) and 6–167 μg/L (average = 49 ± 23 μg/L; Fig. 5B), respectively, under differing flow conditions that ranged from nearly 0 to 11.07 m^3/s over the study period (USGS, 2018). Optical brightener values ranged from 12.51 to 38.04 RFU (average = 21.90 ± 6.63 RFU; Fig. 5C) over the sampling period, and the one $\delta^{11}B$ sample analyzed for Deer Creek had a value of 10.68‰. When comparing F^-, B, and optical brightener data to stream discharge, we observed chemostatic behavior for all tracers ($R^2 \leq 0.01$ and $p \geq 0.28$; Fig. 5). No consistent trends were observed in tracer concentration values across seasons (Fig. 6).

The average drinking water contribution at Deer Creek was 18 ± 18% using the inverse mixing model, which was indistinguishable from the average value derived using the three-component mixing model (17 ± 13%). Since we did not observe any seasonal changes in the municipal water tracers (Fig. 6), the drinking water inputs at this site are most likely the result of leaking infrastructure rather than drinking water applications for lawn irrigation. This inference is based on the expectation that we would see higher drinking water contributions during the summer months when homeowners, parks, and golf courses in the basin more frequently water their lawns.

In contrast to many of the other stream sites across the land use gradient, the average wastewater contribution to the total streamflow at Deer Creek was similar to the drinking water contribution at 15 ± 6% and 14 ± 6% for the inverse and three-component mixing models, respectively. This result indicates higher municipal wastewater inputs from a nearby CSO or more severe wastewater infrastructure leakage in this watershed. However, there are no data available on wet weather CSO volumes or infrastructure leakage rates, so we cannot directly quantify their inputs to Deer Creek.

Interestingly, the relative fractions of our municipal water tracers remained fairly consistent with variable discharge. In other words, we did not observe significant tracer dilution due to event water (Fig. 5), which is known to have low concentrations of our tracers (Hasenmueller and Criss, 2013). We suspect that there are two possible explanations for this observation. First, this site is known to have high inputs of shallow groundwater during flooding conditions (Deeba et al., 2017; Deeba and Hasenmueller, 2018). Shallow groundwater in this catchment is likely highly altered by municipal water signatures. Consequently, if groundwater inputs to the stream remain high even during floods, the municipal water tracers could retain relatively consistent values as a function of discharge. Second, with increasing runoff (and, therefore, increasing event water into the combined sewer system), the contributions of municipal wastewater from the CSO to Deer Creek likely concomitantly increase. The Deer Creek CSO is scheduled for removal (MSD, 2017), so the data shown here can be compared to future water quality analyses to show how effective CSO removal is in improving overall stream and ecosystem quality.

The temporal results from Deer Creek suggest that the relative portions of municipal water inputs to other moderately developed watersheds in our study area could remain constant with discharge. This is likely due to contributions from altered groundwaters, CSOs, or both during high flow conditions. However, in basins with lower groundwater inputs during floods, no combined sewer system, or with different densities of municipal water infrastructure, changes in discharge could affect the relative contributions of municipal waters to streams.

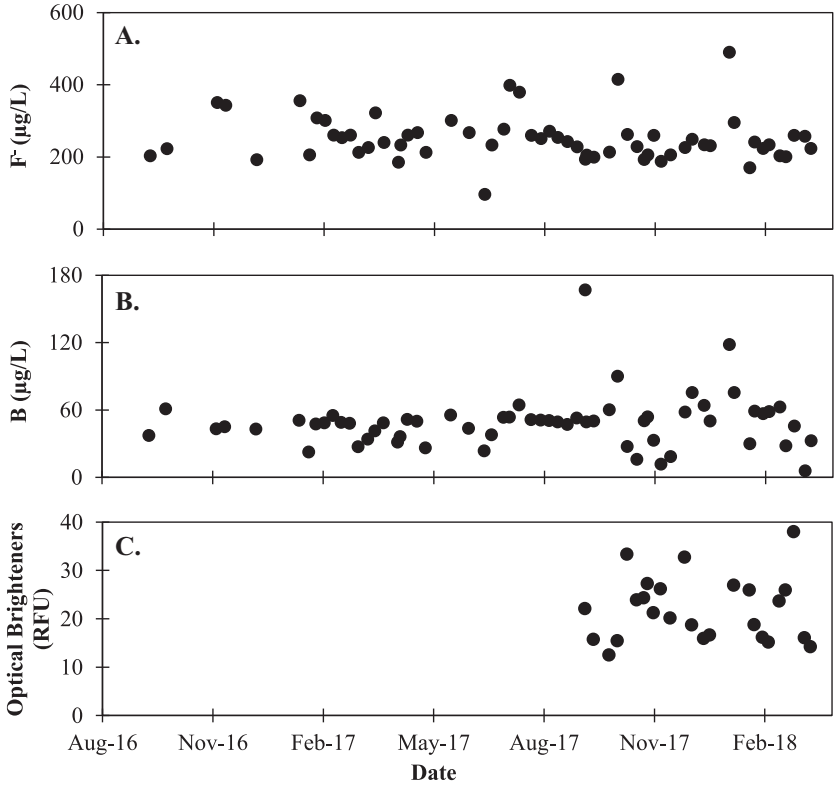

Fig. 6. Levels of (A) F^-, (B) B, and (C) optical brighteners plotted against time at Deer Creek. Note that optical brighteners were only collected from September 2017 to March 2018. No seasonal trends were observed for any of the tracers ($R^2 \leq 0.01$; $p \geq 0.35$).

4. Conclusions

Our multi-tracer approach to distinguish between drinking water and wastewater contributions to urban streams is the first of its kind. Other workers have separated a total municipal water or wastewater signature from that of the natural stream water using chemical tracer approaches. However, further separation into drinking water and wastewater inputs is critical because of the different implications for each of these water types. Large contributions from drinking waters relative to wastewaters may indicate inadequate or failing drinking water-related infrastructure or wasteful lawn irrigation practices. These losses of drinking water to natural stream systems are wasteful of municipal resources and heavily alter urban stream chemistry. Large inputs from wastewaters may be indicative of inadequate infrastructure or inputs from sewer overflows. However, the implications for wastewater releases are of greater concern for human and ecosystem health.

Our study shows that municipal water inputs to streams increase with increasing development. We found that most streams impacted by municipal water contributions are dominated by the drinking water end-member (up to 54% of the total streamflow). Nevertheless, the most highly urbanized streams feature significant wastewater contributions (up to 16% of the total streamflow). We also observed that our municipal tracers did not significantly change with discharge or season. Our techniques will aid in future studies of municipal water inputs to urban stream systems, particularly in quantifying separate contributions of drinking water and wastewater. The use of F^- as a tracer for municipal waters may be applied in any region where fluoridated drinking water is used. Furthermore, dissolved B and optical brighteners are commonly found in detergents; these detergents also have characteristic $\delta^{11}B$ values. The unique signatures of municipal drinking and wastewater aid in the widespread applicability of our multi-tracer method. In regions where municipal end-members do not differ substantially from natural waters (e.g., locations without fluoridated drinking water), our method can be used to constrain their inputs to streams as a function of land use. These types of tracer studies may be beneficial in informing infrastructure improvements in highly urbanized areas and habitat restoration in impacted ecosystems.

Acknowledgements

This work was funded by: (1) research grants to KAL from the Saint Louis University Graduate/Undergraduate Research Collaboration Fund and the Geological Society of America Graduate Student Research Grant Program, (2) research grants to both KAL and EAH from the Litzsinger Road Ecology Center Research Grant Program, and (3) other funds from Saint Louis University. The ICP-OES data for this study were collected on a PerkinElmer Optima 8300 instrument funded by the National Science Foundation (CHE-1626501) and Saint Louis University. We appreciate Susan Baron's help with coordinating field sampling for Deer Creek at the Litzsinger Road Ecology Center. We thank Jennifer Houghton, Rio Febrian, and Heng Chen for assistance with IC, ICP-OES, and MC-ICP-MS analyses, respectively. Special thanks to field and lab assistants Michael Abegg, Camille Buckley, Katie Cassidy, Emily Deeba, Armahni Fearn, Tom Iborg, and David Pan. Jeremy Fine is thanked for his assistance with GIS analyses. We appreciate the help of Frank Genovese, Mike Galluzzo, Dan Richardson, and Steve Bussano from the City of Saint Louis Water Division in collection of drinking water and wastewater samples. We also thank three anonymous reviewers and Damien Guinoiseau whose insightful comments helped us improve this manuscript.

Appendix A. Supplementary data

Supplemental data, including additional end-member descriptions, material and methods, tables, and figures that are mentioned in this paper can be found online at doi:https://doi.org/10.1016/j.scitotenv.2019.03.352.

References

American Society of Civil Engineers (ASCE), 2018. Report card for Missouri's infrastructure, 2018. https://www.infrastructurereportcard.org/state-item/missouri/, Accessed date: 2 October 2018.

Barrett, M.H.; Lerner, D.N.; Hiscock, K.M.; Pedley, S.; Tellam, J.H. The use of marker species to establish the impact of the city of Nottingham, UK on the quantity and quality of its underlying groundwater. In Groundwater in the Urban Environment; Chilton, J. et al. Ed.; Balkema Publications: Rotterdam, The Netherlands, 1997; pp 85–90.

Barth, S., 1998. Application of boron isotopes for tracing sources of anthropogenic contamination in groundwater. Water Res. 32, 685–690.

Barth, S., 2000. Utilization of boron as a critical parameter in water quality evaluation: implications for thermal and mineral water resources in SW Germany and N Switzerland. Environ. Geol. 40, 73–89.

Briand, C., Plagnes, V., Sebilo, M., Louvat, P., Chesnot, T., Schneider, M., Ribstein, P., Marchet, P., 2013. Combination of nitrate (N, O) and boron isotopic ratios with microbiological indicators for the determination of nitrate sources in karstic groundwater. Environ. Chem. 10 (5), 365–369.

Briand, C., Sebilo, M., Louvat, P., Chesnot, T., Vaury, V., Scneider, M., Plagnes, V., 2017. Legacy of contaminant N sources to the NO_3^- signatures in rivers: a combined isotopic ($\delta^{15}N\text{-}NO_3^-$, $\delta^{18}O\text{-}NO_3^-$, $\delta^{11}B$) and microbiological investigation. Sci. Rep. 7, 41703.

Burke, A., Present, T.M., Paris, G., Rae, E.C., Sandilands, B.H., Gaillardet, J., Peucker-Ehrenbrink, B., Fischer, W.W., McClelland, J.W., Spencer, R.G., Voss, B.M., 2018. Sulfur isotopes in rivers: insights into global weathering budgets, pyrite oxidation, and the modern sulfur cycle. Earth Planet Sc. Lett. 2018 (496), 168–177.

Butterwick, L., De Oude, N., Raymond, K., 1989. Safety assessments of boron in aquatic and terrestrial environments. Ecotoxicol. Environ. Saf. 17, 339–371.

Cao, Y., Griffith, J.F., Weisberg, S.B., 2009. Evaluation of optical brightener photodecay characteristics for the detection of human fecal contamination. Water Res. 43, 2273–2279.

Centers for Disease Control and Prevention (CDC). Water fluoridation data and statistics. Fluoridation Statistics. 2014. https://www.cdc.gov/fluoridation/statistics/2014stats.htm (accessed 20 December 2018).

Cheng, K.K., Chalmers, I., Sheldon, T.A., 2007. Adding fluoride to water supplies. BMJ 335 (7622), 699–702.

Chetelat, B., Gaillardet, J., 2005. Boron isotopes in the Seine River, France: a probe of anthropogenic contamination. Environ. Sci. Technol. 8, 2486–2493.

Christian, L.N., Banner, J.L., Mack, L.E., 2011. Sr isotopes as tracers of anthropogenic influence on stream water in the Austin, Texas, area. Chem. Geol. 282, 84–97.

Criss, R.E., Davisson, M.L., Kopp, J.W., 2001. Nonpoint sources in the lower Missouri River. J. Am. Water Works Assoc. 93, 112–122.

Deeba, E.A., Hasenmueller, E.A., 2018. Land Use Controls on Groundwater Inputs to Streams (Abstract): Geological Society of America Abstracts with Programs 50, 6. Indianapolis, Indiana, USA.

Deeba, E.A., Shaughnessy, A.R., Hasenmueller, E.A., 2017. Land Use Controls on Groundwater Inputs and Water Quality for Suburban Streams (Abstract): Geological Society of America Abstracts with Programs 49, 6. Seattle, Washington, USA.

Eiswirth, M., Hötzl, H. The impact of leaking sewers on urban groundwater. In Groundwater in the Urban Environment; Chilton, J. et al. Ed.; Balkema Publications: Rotterdam, The Netherlands, 1997, pp 399–404.

Ellis, J.B., Revitt, D.M., Lister, P., Willgress, C., Buckley, A., 2003. Experimental studies of sewer exfiltration. Water Sci. Technol. 47 (4), 61–67.

Fox, K.K., Daniel, M., Morris, G., Holt, M.S., 2000. The use of measured boron concentration data from the GREATER-ER UK validation study (1996–1998) to generate predicted regional boron concentrations. Sci. Total. Environ. 251/252, 305–316.

Gaillardet, J., Dupre, B., Louvat, P., Allegre, C.J., 1999. Global silicate weathering and CO_2 consumption rates deduced from the chemistry of large rivers. Chem. Geol. 159 (1–4), 3–30.

Gholami, A., Masoum, S., Mohsenikia, A., Abbasi, S., 2016. Chemometrics-assisted excitation-emission fluorescence analytical data for rapid and selective determination of optical brighteners in the presence of uncalibrated interferences. Spectrochim. Acta A 153, 108–117.

Graham, J.L.; Stone, M.L.; Rasmussen, T.J.; Foster, G.M.; Poulton, B.C.; Paxton, C.R.; Harris, T.D. Effects of wastewater effluent discharge and treatment facility upgrades on environmental and biological conditions of Indian Creek, Johnson County, Kansas, June 2004 through June 2013; Scientific Investigations Report 2014–5187; United States Geological Survey, 2014, 78 p.

Grimmond, C.S.B., Oke, T.R., 1986. Urban water balance: 2. Results from a suburb of Vancouver, British Columbia. Water Res. Research 22 (10), 1397–1403.

Guerrot, C., Millot, R., Robert, M., Negrel, P., 2010. Accurate and high-precision determination of boron isotopic ratios at low concentration by MC-ICP-MS (Neptune). Geostand. Geoanal. Res. 35, 275–284.

Guinoiseau, D., Louvat, P., Paris, G., Chen, J.B., Chetelat, B., Rocher, V., Guerin, S., Gaillardet, J., 2018. Are boron isotopes a reliable tracer of anthropogenic inputs to rivers over time? Sci. Total Environ. 626, 1057–1068.

Hagedorn, C., Saluta, M., Hassall, A., Dickerson, J., 2005. Fluorometric Detection of Optical Brighteners as an Indicator of Human Sources of Water Pollution. Part 1: Description and Detection of Optical Brighteners. Virginia Cooperative Extension, Crop and Soil Environmental News.

Hasenmueller, E.A., Criss, R.E., 2013. Multiple sources of boron in urban surface waters and groundwaters. Sci. Total Environ. 447, 235–247.

Hasenmueller, E.A., Robinson, H.K., 2016. Hyporheic zone flow disruption from channel linings: implications for the hydrology and geochemistry of an urban stream, St. Louis, Missouri, USA. J. Earth Sci. 27, 98–109.

Hasenmueller, E.A., Criss, R.E., Winston, W.E., Shaughnessy, A.R., 2017. Stream hydrology and geochemistry along a rural to urban land use gradient. Appl. Geochem. 83, 136–149.

Hayashi, Y., Managaki, S., Takada, H., 2002. Fluorescent whitening agents in Tokyo Bay and adjacent rivers: their application as anthropogenic molecular markers in coastal environments. Environ. Sci. Technol. 36, 3556–3563.
Henckens, M.L.C.M., Driessen, P.P.J., Worrell, E., 2015. Towards a sustainable use of primary boron. Approach to a sustainable use of primary resources. Resour. Conserv. Rey. 103, 9–18.
Homer, C.G., Dewitz, J.A., Yang, L., Jin, S., Danielson, P., Xian, G., Coulston, J., Herold, N.D., Wickham, J.D., Megown, K., 2015. Completion of the 2011 National Land Cover Database for the conterminous United States – representing a decade of land cover change information. Photogramm. Eng. Remote Sensing 81 (5), 345–354.
Jordan, P.R., 1965. Fluvial sediment of the Mississippi River at St. Louis, Missouri; U.S. Geological Survey Water-Supply Paper 1802, U.S. Government Printing Office, Washington, DC (89 p).
Kennedy, M.S., Sarikelle, S., Suravallop, K., 1991. Calibrating hydraulic analyses of distribution systems using fluoride tracer studies. J. Am. Water Works Assoc. 83, 54–59.
Kohn, W.G., Maas, W.R., Malvitz, D.M., Presson, S.M., Shaddix, K.K., 2001. Recommendations for using fluoride to prevent and control dental caries in the United States; Morbid. Mortal. Wkly. Rep. 50 RR-14; Department of Health and Human Services, Centers for Disease Control and Prevention, U.S. Government Printing Office, Washington, DC.
Lee, E.S., Krothe, N.C., 2001. A four-component mixing model for water in a karst terrain in south-central Indiana, USA. Using solute concentration and stable isotopes as tracers. Chem. Geol. 179, 129–143.
Lennon, M.A., Whelton, H., O'Mullane, D., Ekstrand, J., 2004. Rolling revision of the WHO guidelines for drinking-water quality: fluoride. World Health Organization.
Lerner, D.N., 2002. Identifying and quantifying urban recharge: a review. Hydrogeol. J. 10, 143–152.
Lockmiller, K.A. 2018. Using multiple tracers to distinguish between municipal drinking water and wastewater inputs to urban streams. Masters thesis, Saint Louis University.
Meenakshi, A., Maheshwari, R.C., 2006. Fluoride in drinking water and its removal. J. Hazard. Mater. 137, 456–463.
Metropolitan St. Louis Sewer District (MSD), 2017. About MSD Project Clear. http://www.projectclearstl.org/about/ (accessed Mar 10, 2017).
Missouri American Water, Missouri River-derived drinking water distribution area geospatial data, personal communication, 2016.
Motiee, H., McBean, E., Motiei, A., 2007. Estimating physical unaccounted for water (UFW) in distribution networks using simulation models and GIS. Urban Water J. 4, 43–52.
Negrel, P., Allegre, C.J., Dupre, B., Lewin, E., 1993. Erosion sources determined by inversion of major and trace element ratios in river water: the Congo Basin case. Earth Planet. Sc. Lett. 120, 59–76.
Noireaux, J., Gaillardet, J., Sullivan, P.L., Brantley, S.L., 2014. Boron isotope fractionation in soils at Shale Hills CZO. Proced. Earth Plan. Sc. 10, 218–222.
Passarello, M.C., Sharp Jr., J.M., Pierce, S.A., 2012. Estimating urban-induced artificial recharge: a case study for Austin. TX. Environ. Engin. Geosci. 18, 25–36.
Petelet-Giraud, E., Klaver, G., Negrel, P., 2009. Natural versus anthropogenic sources in the surface- and groundwater dissolved load of the Dommel River (Meuse basin): constraints by boron and strontium isotopes and gadolinium anomaly. J. Hydrol. 369 (3–4), 336–349.
Poiger, T., Field, J.A., Field, T.M., Siegrist, H., Giger, W., 1998. Behavior of fluorescent whitening agents during sewage treatment. Water Res. 32, 1939–1947.
Reardon, E.J., Wang, Y., 2000. A limestone reactor for fluoride removal from wastewaters. Environ. Sci. Technol. 34, 3247–3253.
Robinson, H.K., Hasenmueller, E.A., 2017. Transport of road salt contamination in karst aquifers and soils over multiple timescales. Sci. Total Environ. 603-604, 94–108.
Robinson, H.K., Hasenmueller, E.A., Chambers, L.G., 2017. Soils as a reservoir for road salt retention leading to its gradual release to groundwater. Appl. Geochem. 83, 72–85.
Roy, S., Gaillardet, J., Allegre, C.J., 1999. Geochemistry of dissolved and suspended loads of the Seine River, France: anthropogenic impact, carbonate and silicate weathering. Geochim. Cosmochim. Ac. 63 (9), 1277–1292.
Rutsch, M., Rieckermann, J., Krebs, P., 2006. Quantification of sewer leakage: a review. Water Sci. Technol. 54 (6–7), 135–144.
Stueber, A.M., Criss, R.E., 2005. Origin and transport of dissolved chemicals in a karst watershed, southwestern Illinois. J. Am. Water Resour. Assoc. 41, 267–290.
Tavares, M.E., Spivey, M.I.H., McIver, M.R., Mallin, M.A., 2008. Testing for optical brighteners and fecal bacteria to detect sewage leaks in tidal creeks. J. N. C. Acad. Sci. 124, 91–97.
Torres, M.A., West, A.J., Clark, K.E., Paris, G., Bouchez, J., Ponton, C., Feakins, S.J., Galy, V., Adkins, J.F., 2016. The acid and alkalinity budgets of weathering in the Andes-Amazon system: insights into the erosional control of global biogeochemical cycles. Earth Planet. Sc. Lett. 450, 381–391.
United Nations Department of Economics and Social Affairs (UNDESA), 2016. The World's Cities in 2016 Data Booklet, Population Division. http://www.un.org/en/development/desa/population/publications/pdf/urbanization/the_worlds_cities_in_2016_data_booklet.pdf (accessed 7 March 2018).
United States Environmental Protection Agency (USEPA), 2018a. Water Sense: Outdoor water use in the United States. https://19january2017snapshot.epa.gov/www3/watersense/pubs/outdoor.html (accessed 2 October 2018).
United States Environmental Protection Agency (USEPA), 2018b. St. Louis Clean Water Act settlement. https://www.epa.gov/enforcement/st-louis-clean-water-act-settlement#main-content, Accessed date: 7 March 2018.
United States Geological Survey (USGS), 2012. Mineral commodity summaries.
United States Geological Survey (USGS), 2018. Daily streamflow conditions. https://waterdata.usgs.gov/mo/nwis/rt (accessed 11 March 2018).
Vengosh, A., Heumann, K.G., Juraske, S., Kasher, R., 1994. Boron isotope application for tracing sources of contamination in groundwater. Environ. Sci. Technol. 28, 1968–1974.
Vollertsen, J., Hvitved-Jacobsen, T., 2003. Exfiltration from gravity sewers: a pilot scale study. Water Sci. Technol. 47 (4), 69–76.
Widory, D., Kloppmann, W., Chery, L., Bonnin, J., Rochdi, H., Guinamant, J.-L., 2004a. Nitrate in groundwater: an isotopic multi-tracer approach. J. Contam. Hydrol. 72 (1–4), 165–188.
Widory, D., Petelet-Giraud, E., Negrel, P., Ladouche, B., 2004b. Tracking the sources of nitrate in groundwater using coupled nitrogen and boron isotopes: a synthesis. Environ. Sci. Technol. 39 (2), 539–548.
Widory, D., Petelet-Giraud, E., Negrel, P., Ladouche, B., 2005. Tracking the sources of nitrate in groundwater using coupled nitrogen and boron isotopes: a synthesis. Environ. Sci. Technol. 39 (2), 539–548.
Xian, G., Homer, C., Dewitz, J., Fry, J., Hossain, N., Wickham, J., 2011. The change of impervious surface area between 2001 and 2006 in the conterminous United States. Photogramm. Eng. Remote Sensing 77 (8), 758–762.
Xu, Z., Wang, L., Yin, H., Li, H., Schwegler, B.R., 2016. Source apportionment of non-stormwater entries into storm drains using marker species: modeling approach and verification. Ecol. Indic. 61, 546–557.
Yin, H., Xie, M., Zhang, L., Huang, J., Xu, Z., Li, H., Jian, R., Wang, R., Zeng, X., 2019. Identification of sewage markers to indicate sources of contamination: low cost options for misconnected non-stormwater source tracking in stormwater systems. Sci. Total Environ. 648, 125–134.